# The Excited-State Chemistry of Protochlorophyllide a: A Time-Resolved Fluorescence Study

**ARTICLE** *in* CHEMPHYSCHEM · AUGUST 2006

Impact Factor: 3.42 · DOI: 10.1002/cphc.200600172 · Source: PubMed



**9 AUTHORS**, INCLUDING:

Wolfgang Kiefer
University of Wuerzburg
**878** PUBLICATIONS **9,847** CITATIONS
SEE PROFILE

Peter Schellenberg
University of Minho
**37** PUBLICATIONS **375** CITATIONS
SEE PROFILE

Paulius Grigaravicius
German Cancer Research Center
**17** PUBLICATIONS **154** CITATIONS
SEE PROFILE

Juergen Popp
Friedrich Schiller University Jena
**407** PUBLICATIONS **6,061** CITATIONS
SEE PROFILE

DOI: 10.1002/cphc.200600172

# The Excited-State Chemistry of Protochlorophyllide a: A Time-Resolved Fluorescence Study

Benjamin Dietzek,[a, b] Wolfgang Kiefer,[a] Arkady Yartsev,[b] Villy Sundström,[b] Peter Schellenberg,[c] Paulius Grigaravicius,[c] Gudrun Hermann,[d] Jürgen Popp,[e] and Michael Schmitt*[e]

*The excited-state processes of protochlorophyllide a, the precursor of chlorophyll a in chlorophyll biosynthesis, are studied using picosecond time-resolved fluorescence spectroscopy. Following excitation into the Soret band, two distinct fluorescence components, with emission maxima at 640 and 647 nm, are observed. The 640 nm emitting component appears within the time resolution of the experiment and then decays with a time constant of 27 ps. In contrast, the 647 nm emitting component is built up with a 3.5 ps rise time and undergoes a subsequent decay with a time constant of 3.5 ns. The 3.5 ps rise kinetics are attributed to relaxations in the electronically excited state preceding the nanosecond fluorescence, which is ascribed to emission out of the thermally equilibrated $S_1$ state. The 27 ps fluorescence, which appears within the experimental response of the streak camera, is suggested to originate from a second minimum on the excited-state potential-energy surface. The population of the secondary excited state is suggested to reflect a very fast motion out of the Franck–Condon region along a reaction coordinate different from the one connecting the Franck–Condon region with the $S_1$ potential-energy minimum. The 27 ps-component is an emissive intermediate on the reactive excited-state pathway, as its decay yields the intermediate photoproduct, which has been identified previously (J. Phys. Chem. B **2006**, 110, 4399–4406). No emission of the photoproduct is observed. The results of the time-resolved fluorescence study allow a detailed spectral characterization of the emission of the excited states in protochlorophyllide a, and the refinement of the kinetic model deduced from ultrafast absorption measurements.*

## Introduction

Protochlorophyllide a (Pchlide a) belongs to the plant tetrapyrroles, which are of significant biological importance. As a porphyrin-like compound, made up of four pyrrole-type rings linked together by four methine bridges (Figure 1), Pchlide a is a precursor of chlorophyll a in chlorophyll biosynthesis. In the biosynthetic pathway of chlorophyll, Pchlide a is synthesized from 5-aminolevulinic acid in a sequence of enzyme-catalyzed reactions. In a subsequent step, Pchlide a is reduced at the C17/C18 double bond of ring D to yield the chlorin macrocycle of chlorophyllide a.[1–5] The reduction is catalyzed by the enzyme nicotinamide adenine dinucleotide phosphate, (NADPH):protochlorophyllide oxidoreductase (POR), EC 1.3.1.33, which exists as a ternary complex with the substrate, Pchlide a, and the coenzyme, NADPH, in all oxygenic photosynthetic organisms.[6–9] This enzymatic reduction of Pchlide a represents a key regulatory step in the synthesis of chlorophyll and the sub-

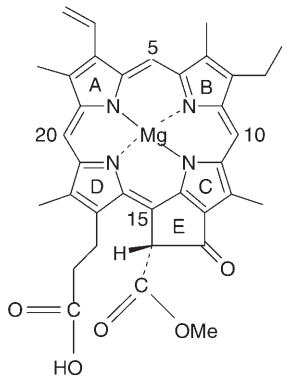


**Figure 1.** Chemical structure of protochlorophyllide a.

[a] *Dr. B. Dietzek, Prof. Dr. W. Kiefer*
*Institut für Physikalische Chemie*
*Bayerische Julius-Maximilians-Universität Würzburg*
*Am Hubland, 97074 Würzburg (Germany)*

[b] *Dr. B. Dietzek, Dr. A. Yartsev, Prof. Dr. V. Sundström*
*Department of Chemical Physics, Lund University*
*P.O. Box 124, 22100-Lund (Sweden)*

[c] *Dr. P. Schellenberg, Dr. P. Grigaravicius*
*Institut für Molekulare Biotechnolgie Jena*
*Beutenbergstraße 11, 07745 Jena (Germany)*

[d] *Dr. G. Hermann*
*Institut für Biochemie und Biophysik*
*Friedrich-Schiller-Universität Jena, Philosophenweg 12*
*07743 Jena (Germany)*

[e] *Prof. Dr. J. Popp, Dr. M. Schmitt*
*Institut für Physikalische Chemie*
*Friedrich-Schiller Universität Jena, Helmholtzweg 4*
*07743 Jena (Germany)*
*Fax: (+49) 3641-948-300*
*E-mail: m.schmitt@uni-jena.de*

  

sequent assembly of the photosynthetic apparatus, because the POR requires light for the initiation of the enzymatic activity.[10–12] The photoregulation ensures that tetrapyrrolic intermediates do not accumulate and cause photosensitized side reactions. Apart from the regulatory effect on chlorophyll biosynthesis, the enzyme POR exhibits another interesting feature in that it is one of only two enzymes in which catalytic activity is switched on by the absorption of light. The requirement for light makes the POR an attractive model for studying the primary events of an enzymatic reaction in real time by use of time-resolved spectroscopy. Given this background, a first femtosecond study on the ultrafast steps of the enzymatic reaction was reported recently.[13] The experimental results were interpreted in terms of a complex mechanism with two parallel reactions leading to the formation of chlorophyllide a on the time scale of 3 ps and 400 ps, respectively. In order to obtain further information that could help us understand the complex photochemical reaction in the POR enzyme, we initiated a study on the excited-state dynamics of Pchlide a alone in solution, separated from the POR apoprotein. In two recent papers, we have presented a model for the reaction dynamics in excited Pchlide a that accounts for the results of time-resolved absorption measurements carried out in solvents of different polarity, viscosity, and protic/aprotic properties.[14,15] According to this model, the initial excited-state population decays via vibrational relaxation/cooling within 4 ps into the fully relaxed (cold) $S_1$ excited state, which in turn undergoes relaxation back into the ground state with a comparatively slow time constant of 3.5 ns. In addition, a second decay path, which leads to the formation of an intermediate photoproduct, is available in polar solvents. From the polarity-controlled deactivation via the second decay channel, it is suggested that the intermediate photoproduct represents an intramolecular charge-transfer state ($S_{ICT}$), which most probably results from the electron-withdrawing effect of the cyclopentanone ring attached directly to the $\pi$-electron conjugation path of the porphyrin macrocycle.[14] In the nonpolar solvent case, the $S_{ICT}$ state seems to be higher in energy compared to the situation in polar solvents, so that the $S_{ICT}$ state is not populated upon photoabsorption in the $Q_{00}$ band, and only the $S_1$ state dynamics can be observed. A distinct spectral characterization of the excited-state manifold involved in the complex relaxation processes of photoexcited Pchlide a by transient absorption spectroscopy is hampered by the observation of broad and basically featureless photoinduced absorption bands.[14,15] Thus, we expand on this earlier work by exploring the time-resolved fluorescence kinetics of Pchlide a. From an emission study like this, we expect to classify the emission spectra of the individual excited state(s) in detail, and thus gain yet more reliable insights into the excited-state chemistry of Pchlide a.

## Results

### Stationary Absorption and Fluorescence Spectra

As a background for the time-resolved fluorescence measurement, the static spectroscopic properties of Pchlide a are summarized below. Figure 2 displays the steady-state absorption spectrum of Pchlide a in methanol and, in addition, the steady-state fluorescence and fluorescence excitation spectrum. The absorption spectrum shows an intense Soret band with a peak at 434 nm and three much weaker Q-absorption bands with peaks at 534, 576, and 629 nm. These spectral features are representative of the absorption spectra of porphyrins.[16] In particular, they agree very well with the spectral characteristics reported recently for Pchlide a in different organic solvents.[17] The fluorescence spectrum exhibits a strong $S_1 \rightarrow S_0$ band centered at 641 nm as well as a shoulder at 690 nm. The appearance of a longwave shoulder in the fluorescence spectrum is common in the emission characteristics of porphyrins, and is typically attributed to vibronic progression. The fluorescence spectrum is only slightly red shifted relative to the absorption spectrum, with a small Stokes shift of $\approx 300\ cm^{-1}$, indicating the minor role of solvent reorganization effects on the $S_1 \rightarrow S_0$ transition. Further, the fluorescence spectrum does not depend on the excitation wavelength, and the excitation spectrum and the absorption spectrum are virtually superimposed. This finding suggests that only one type of Pchlide a species exists in the ground state.

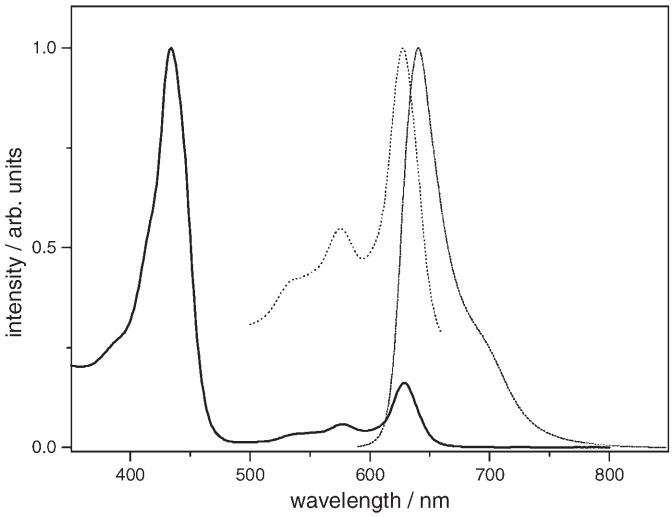


**Figure 2.** Steady-state absorption (——), fluorescence (•••••) as well as fluorescence excitation spectrum (– – –) of protochlorophyllide a in methanol. The fluorescence spectrum (scaled) is shown for excitation at 627 nm, and the fluorescence excitation spectrum for the emission at 641 nm. The fluorescence excitation spectrum has been scaled and offset for clarity.

### Time-Resolved Fluorescence Experiments

Figure 3 A shows the time evolution of the fluorescence spectra obtained at different times after excitation of Pchlide a into the Soret band at 435 nm. The spectra reveal a clear red shift in the position of the fluorescence maximum with increasing delay time. While the fluorescence peak is centered at 644 nm at short time delays, it is gradually shifted into the red spectral region as the delay time is increased, appearing finally at 651 nm after 600 ps. In contrast to the main fluorescence

  

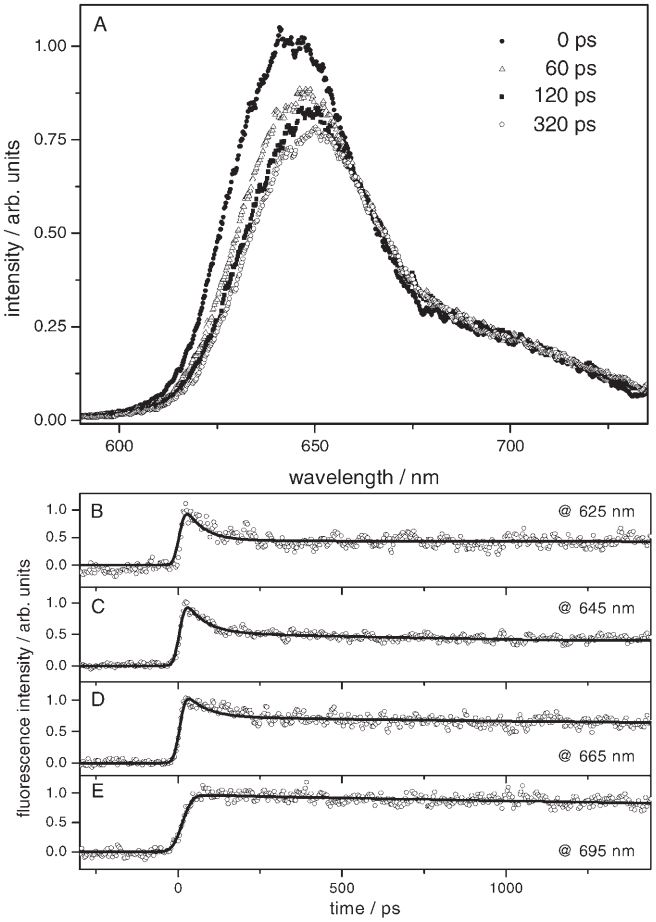


**Figure 3.** Time-resolved fluorescence spectra of protochlorophyllide a in methanol and fluorescence kinetics measured at selected probe wavelengths with a time resolution of 40 ps. A) Fluorescence spectra as a function of time after Soret band excitation at 435 nm. For experimental reasons, the times are given with respect to the time for the appearance of the intensity maximum at 641 nm. B–E) Fluorescence kinetics measured at the four probe wavelengths indicated after excitation at 435 nm. Experimentally measured data (○); calculated functions from the best-fit parameters (——). The estimated time constants are $\tau_1 = 40$ ps, $\tau_2 = 3.3$ to 3.5 ns, depending on the specific probe wavelength.

band, which loses intensity with time, the intensity of the shoulder at $\approx 700$ nm does not considerably vary with time over the first 320 ps after photoabsorption. This effect is unexpected, on the basis of the common observation of a shoulder in the emission spectra of porphyrins reflecting the vibronic progression of the $S_1 \rightarrow S_0$ transition, in which case the shoulder would be expected to decay in parallel with the fundamental transition. Furthermore, the absence of a rise component on a time-scale comparable to the decay in the main transition, pointing to relaxation within the electronically excited state, indicates that the observed kinetics cannot be explained in terms of vibrational cooling, intramolecular vibrational energy redistribution (IVR), or solvation dynamics. These findings rather suggest the contribution of a long-lived fluorescence component, which dominates the fluorescence decay in the red ($\approx 700$ nm) spectral region, whereas a comparatively short lifetime fluorescence component dominates the blue part of the spectrum. For a more detailed kinetic analysis, the time evolution of the fluorescence is examined at different wavelengths across the emission band (by cutting the three-dimensional records of the streak camera along the time axis). In Figures 3 B–E, the kinetics are shown for four selected emission wavelengths at a time resolution of 40 ps (full width at half maximum, FWHM). The fluorescence at 695 nm, a wavelength in the spectral region of the red shoulder, is seen to appear within the apparatus temporal response and then remains quasiconstant, obviously owing to the contribution from a very long-lived component. Unlike the kinetics at 695 nm, the kinetic profiles monitored at 625, 645, and 665 nm, that is, at wavelengths across the main fluorescence band, reveal a fast decay subsequent to the initial instrument-response limited rise, followed by a long-time decay as detected at 695 nm. The kinetics at the different emission wavelengths fit well to a double-exponential function convoluted with the instrument-response function. The two time constants that result from this approach are $\tau_1 \leq 40$ ps and $\tau_2 \geq 3.0$ ns. Their contributions to the overall kinetics, however, are dependent on the emission wavelengths. While the decay amplitude of the $\leq 40$ ps component approaches zero at the lowest energy probe wavelength of 695 nm, it increases up to 64% at 625 nm (the shortest probe wavelength). For a closer examination of the time constant $\tau_2$, the fluorescence kinetics are measured over a longer time interval, up to 20 ns, more adequate to the $\geq 3.0$ ns decay time. The data acquisition up to 20 ns after excitation thus yields a value of $3.4 \pm 0.1$ ns, in excellent agreement with the 3.5 ns fluorescence lifetime found for Pchlide a in methanol by phase fluorimetry.[17]

To facilitate a yet more accurate determination of the time constant $\tau_1$ in our experiments, the fluorescence kinetics are re-examined at a higher time resolution of 2 ps (FWHM). Figure 4 shows the fluorescence kinetics recorded after Soret band excitation at 398 nm. The fluorescence measured at 600 to 630 nm (Figure 4 A), that is, at the short wavelength tail of the fluorescence band, gives a kinetic profile similar to that depicted in Figure 3 B. Following an initial, instrument-response limited rise, the fluorescence decay has an emission temporal behavior best fitted by two distinct kinetic components. The main component with the largest contribution (67%) has a lifetime of 27 ps, and obviously corresponds to the $\leq 40$ ps component identified less accurately in the above experiments at lower time resolution (40 ps FWHM). The smaller component fits to a lifetime of $\geq 3.0$ ns, which correlates with the $3.4 \pm 0.1$ ns lifetime determined more accurately at the lower time resolution. A completely different kinetic profile is obtained when the fluorescence is observed at 660–700 nm, that is, in the red shoulder of the $S_1 \rightarrow S_0$ emission. As can be seen from Figure 4 B, a fit including two decay functions deconvoluted from the system temporal response, as done above, clearly fails to approach the experimental data. Instead, a good fit requires a rise term, given by the factor $1 - \exp(-t/\tau_{rise})$ in the fit function. Accordingly, on the basis of the best-fit results, the kinetics comprise of a 3.5 ps rise component and the longest-decay component of $\geq 3.0$ ns. This result strongly suggests that the nanosecond fluorescence is built up with a 3.5 ps rise time, whereas in the kinetics at 600–630 nm, the 27 ps fluores-

  

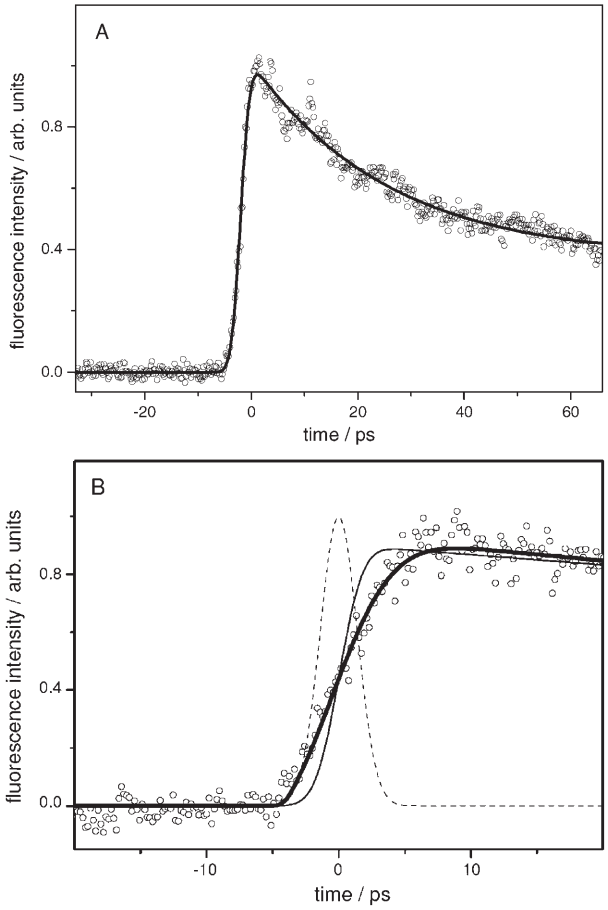


**Figure 4.** Fluorescence kinetics of protochlorophyllide a in methanol measured with a time resolution of 2 ps after Soret band excitation at 398 nm. A) Fluorescence kinetics monitored in the wavelength region 600–630 nm. Experimentally measured data (○); best-fit function (——). B) Fluorescence kinetics measured in the wavelength region 660–700 nm. For comparison, the experimentally measured data (○), the experimental response function (– – –), the fit including a 3.5 ps rise time (——), and the fit with no initial rise (grey line) are shown.

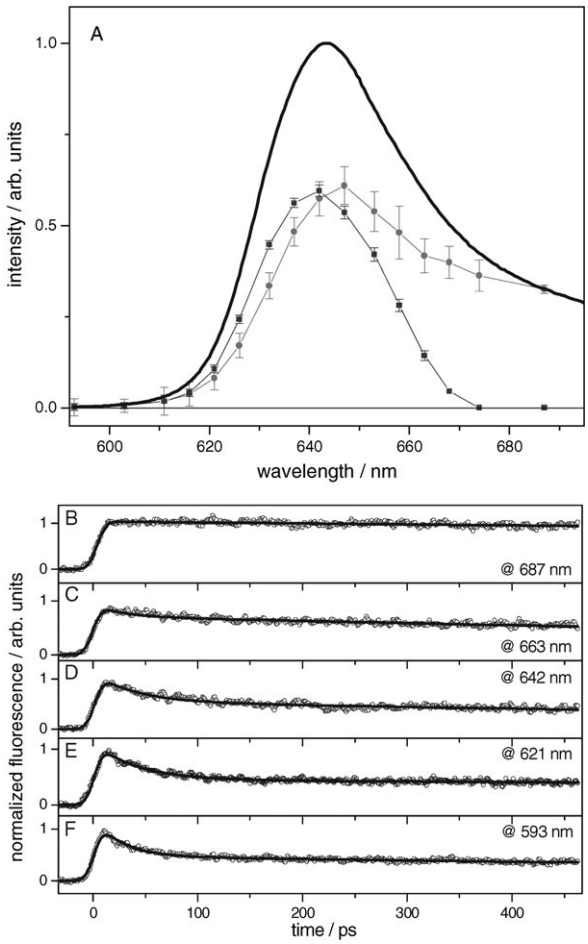


**Figure 5.** Decay-associated fluorescence spectra of the 27 ps (■) and 3.5 ns (●) components and kinetic traces at representative probe wavelengths. A) Decay-associated fluorescence spectra as determined from the fluorescence kinetics at different probe wavelengths. The steady-state fluorescence spectrum (——) is shown for comparison. B–F) Kinetic traces of fluorescence transients measured at characteristic probe wavelengths. Experimentally measured data (○); calculated functions from the best-fit parameters (——).

cence appears within the time resolution of the experimental setup and exhibits no initial rise time.

Figure 5 A shows the decay-associated spectra (DAS) of the 27 ps and the 3.4 ns components, as calculated from the fluorescence decays at the different emission wavelengths. Figure 5 B summarizes representative kinetic traces in order to illustrate the main features of the two spectra. The DAS of the 27 ps component has an emission maximum at 640 nm and a Gaussian width of about 580 $cm^{-1}$. It reflects a symmetric transition exhibiting no vibronic structure. In comparison, the maximum in the DAS of the 3.4 ns component is slightly red shifted to 647 nm, which represents an energetic difference in the emission maxima of 170 $cm^{-1}$. The 3.4 ns spectrum extends over the entire spectral range examined in our fluorescence experiments with its relative contribution being higher than that of the 27 ps component at wavelengths longer than 640 nm. In contrast, the relative contribution of the 27 ps component dominates at wavelengths shorter than 640 nm and drops off to zero at wavelengths longer than 670 nm. This spectral characterization of the two components is in full agreement with the above observation (Figure 3) that the fluorescence decays measured near the maximum of the 0–0 transition and in the red shoulder of the $S_1$ emission band do not correlate with each other, with the decay being considerably slower at the low versus the high-energy edge of the emission band.

## Discussion

The discussion of our experimental results starts from the observation of two spectrally distinct fluorescence components, whose emission maxima are separated by only 170 $cm^{-1}$. While the blue emissive state (emission maximum at 640 nm) appears instantaneously and decays with a 27 ps lifetime, the red emissive state (emission maximum at 647 nm) is found to have a nanosecond lifetime and exhibits a rise-time of 3.5 ps. This rise component is assigned to cooling of the initially hot $S_1$ state. A similar 4 ps kinetic component is present in the transient-absorption data, and its spectral characteristics are consistent with assigning it to vibrational relaxation in the electroni-

  

cally excited state.[14,15] Both vibrational cooling and solvation dynamics might contribute to the vibrational process, while contributions of IVR can be excluded on the basis of the relatively long timescale of the observed process.[18,19] The fact that no 27 ps rise is recorded over the entire spectral range of the experiment, detecting emission up to 730 nm corresponding to only about 10% of the maximum fluorescence intensity, indicates that the depopulation of the blue emissive state is not coupled to the formation of another emissive state. In particular, the decay of the blue emissive state does not result in the formation of the red emissive state with the nanosecond lifetime. The conclusion of distinct, separated emissive states is corroborated by the decay-associated spectra constructed from the transient absorption data, that clearly show distinct spectral features for the cooling and the 27 ps component.[14] The 27 ps component with the fluorescence slightly blue-shifted from the long-lived nanosecond component most likely belongs to a second local minimum on the excited-state surface ($S_x$). As evidenced by the peaks in the corresponding decay-associated fluorescence spectra (Figure 5A) the $S_X$ emission maximum appears about 170 $cm^{-1}$ blue shifted from the emission of the fully relaxed $S_1$ state. On the basis of the insensitivity of the steady-state fluorescence spectrum on the excitation energy, and the finding of identical fluorescence excitation spectra for various detection wavelengths, it is concluded that only a single type of Pchlide a ground-state species exists (see above). Thus, excluding the existence of a secondary ground-state minimum, and assuming that the optimal Franck–Condon (FC) factors of emission can be related to the lowest vibronic level in the respective excited state, the energetic separation of the $S_x$ state from the fully relaxed $S_1$ state can be estimated to 170 $cm^{-1}$. This remarkably small energy difference between the two emission maxima compared to the thermal energy at room temperature ($kT_{room} \approx 200\ cm^{-1}$) hints at the presence of a barrier separating the population in the $S_1$ and $S_x$ states. In the absence of such a barrier, one would not expect to observe distinct spectral and temporal characteristics in the emission of the two states, because in this case the thermal energy is sufficient to move the population between the two local minima on the excited-state surface. This argument is strengthened when recalling that the spectral temperature defined as the average energy per vibration following photoexcitation is even higher than room temperature. Nonetheless, the assumption of a high barrier separating the $S_1$ from the $S_x$ state is intriguing when contrasted with the experimental finding of the ultrafast population of the $S_x$ state. The population of the $S_X$ state from the initially excited state cannot be temporally resolved, either in the fluorescence measurements with an experimental response of 2 ps (FWHM), or in the absorption experiments with a time resolution of 100 fs. This process is therefore expected to occur in less than 100 fs, since a rise time of more than 100 fs should have been detected at least in our absorption measurements.[14,15] Assuming the direct population of the $S_1$ state upon photoabsorption, a high barrier would lead to a much slower population of the $S_x$ state on a timescale detectable within our absorption experiments. Thus, the spectral characterization of the Pchlide a fluorescence points to the importance of a second orthogonal reaction coordinate on the excited-state surface. The small energetic difference between the emission maxima, together with the instantaneous population of the $S_x$ state, can be rationalized in the framework of a model in which a FC active absorption manifold is separated from two distinct emissive local minima on the excited-state surface. Following this argument, photoabsorption promotes Pchlide a molecules to the FC point of the excited state (Figure 6). From this point, photoexcited Pchlide a molecules relax ultrafast in a branching reaction into the vibrationally hot $S_1$ state and into the $S_x$ potential minimum. These two states are separated along two different reaction coordinates (labeled $x_r$ and $x_{nr}$, pointing to the reactive and nonreactive nature of the excited-state pathways, respectively). As outlined above, the motion out of the FC point is extremely fast, and escapes detection in the present fluorescence

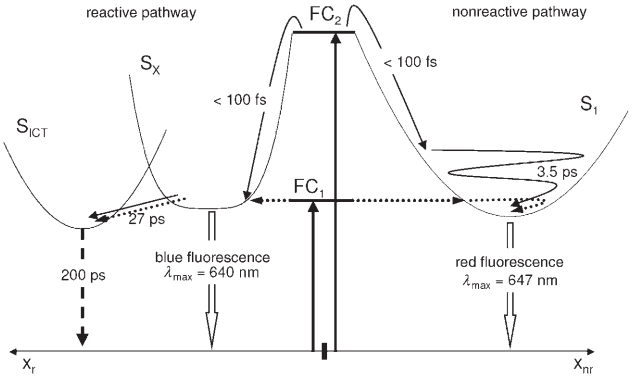


**Figure 6.** Energy-level diagram of the excited-state dynamics of Pchlide a after Soret band excitation. $FC_2$ refers to the FC region in the Soret band, and $FC_1$ refers to the FC region in the $Q_{00}$-band. The thin solid arrows refer to processes present in the time-resolved fluorescence data; the dotted arrows refer to the excited-state relaxation as it appears upon photoexcitation into the $Q_{00}$ band. The reactive ($x_r$) and nonreactive coordinates ($x_{nr}$) are suggested to be orthogonal. Their representation along a single dimension is due to pictorial simplicity.

experiments owing to the insufficient time resolution which can be attained by the streak camera setup. Therefore, to monitor the transition from the FC point to the $S_X$ state, further experiments with improved time resolution are required. Like the population kinetics of the $S_X$ state, the timescale of the $S_2 \rightarrow S_1$ transition is also beyond the time resolution of the fluorescence experiments, since, apart from the 3.5 ps rate for vibrational relaxation/cooling, no additional rise time is detectable in the fluorescence kinetics. The accordingly fast $S_2 \rightarrow S_1$ relaxation is in line with estimates of sub-100 fs reported for the Soret lifetime of Zn, Mg, and free base porphyrins.[20–22]

It is worth noting that, in contrast to the long-lived red fluorescence, the 27 ps fluorescence is virtually unaffected by cooling. That is, no rise-component is observed in the blue emissive band. This result indicates that the motion out of the FC point along the reactive coordinate occurs on a steeper potential-energy surface compared to the relaxation into the $S_1$ state along the nonreactive coordinate. Nonetheless, the decay of

  

the $S_x$ state could be followed in detail, and occurs with a 27 ps time constant. The $S_x$ characteristics obtained from the present time-resolved fluorescence study agree with the findings of our previous absorption experiments.[14,15] However, the model that accounts for the transient-absorption data invokes the presence of an additional intermediate photoproduct state. Owing to the dependence of the excited-state dynamics on the solvent polarity, the photoproduct state is assigned to $S_{ICT}$, which is lower in energy than the $S_1$ excited state in a polar environment. Similar intramolecular charge transfer states have been described in a series of some highly substituted carotenoids.[23] In Pchlide a, the dipolar nature of the $S_{ICT}$ is expected to result from the presence of the cyclopentanone ring, in particular the carbonyl group of this ring, which is attached as an electron-withdrawing group directly to the conjugated $\pi$-electron path of the porphyrin macrocycle. As seen in the absorption measurements, the $S_{ICT}$ state appears with a rise time of 27 ps and decays back to the original ground state with a time constant of 200 ps. The absence of a fluorescence counterpart to the 200 ps decay time suggests that the $S_{ICT}$ state is nonemissive, possibly owing to the strongly reduced dipole moment associated with the charge-transfer character of this state. Nonetheless, the possibility that emission from the $S_{ICT}$ state occurs at wavelengths longer than 750 nm, which cannot be assessed in our experimental observation window, cannot be excluded.

#### Model of the Excited-State Dynamics

On the basis of the experimental data presented here, and following the above arguments, the observed fluorescence kinetics allow us to refine the previously suggested model for the de-excitation of electronically excited Pchlide a via two distinct decay channels,[14,15] and to gain a more detailed insight into the energy landscape of the excited states involved. The central finding of this work, the presence of two distinct emissive states with closely spaced emission maxima, points to the presence of a complex excited-state surface of Pchlide a, on which the absorption FC point is separated from either of the two emissive states by two most likely orthogonal reaction coordinates. Following the nonreactive channel (Figure 6), the vibrationally hot $S_1$ state is rapidly formed upon photoexcitation and depopulated by a 3.5 ps process, representing vibrational relaxation and solvation dynamics, to the thermally equilibrated $S_1$ state. The cold $S_1$ state is nonreactive and undergoes relaxation into the original ground state within 3.4 ns. In competition with the nonreactive path, an ultrafast excited-state motion along a steep reaction coordinate out of the FC region into the secondary excited state, $S_X$, takes place. The $S_X$ state is then responsible for the reactive part in the photochemistry of Pchlide a, in that it facilitates the formation of an intermediate photoproduct state ($S_{ICT}$), which is nonemissive and most likely represents an intramolecular charge–transfer state. In a final step, the intermediate photoproduct undergoes relaxation back into the original ground state with a time constant of 200 ps.

At the present stage of our study, it remains unknown along which reaction coordinates the initial relaxation out of the FC region and the branching into the reactive and nonreactive pathways occurs. However, it is worth noting that the reduction of Pchlide a to chlorophyllide a by the enzyme POR was reported to proceed in two parallel reactions with time constants of 3 and 400 ps.[13] From the close similarity of the 400 ps time constant and the 200 ps lifetime of the intermediate $S_{ICT}$ state, it is tempting to speculate that the enzymatic reaction also proceeds via the formation of an intramolecular charge–transfer state, which may precede the reduction of the porphyrin to the chlorin macrocycle. This hypothesis is further supported by the results of a low-temperature study on the initial photochemistry in the enzyme POR.[24,25] In these experiments, a nonfluorescent intermediate was discovered as a first photoproduct at temperatures as low as 120 K, and was suggested to represent an intermolecular charge-transfer complex, which itself was thought to arise from a photoinduced charge separation across the Pchlide molecule.[26,27]

## Conclusions

This paper presents a time-resolved fluorescence study of Pchlide a, the porphyrin-like substrate of the enzyme protochlorophyllide oxidoreductase. The results allow for a detailed spectral characterization of the emissive excited states in Pchlide a. The fluorescence data obtained upon excitation in the Soret band show the presence of two distinct emission bands with lifetimes of 27 ps and 3.4 ns. In the decay-associated fluorescence spectrum, the 27 ps component originating from the $S_x$ state has a peak at 640 nm, while the fluorescence peak of the nanosecond ($S_1$) component is positioned at 647 nm. The two fluorescence components match, to a high degree, the kinetic components identified in the time-resolved absorption experiments after Q-band excitation.[14] Nonetheless, a detailed spectral characterization of these two states in time-resolved absorption experiments is hampered by the congestion of broad and featureless photoinduced absorption bands.

The results of the time-resolved fluorescence study significantly refine the model describing the excited-state processes of Pchlide a in terms of a branching of the initially excited-state population into a reactive and a nonreactive path. These data further allow for a more detailed spectral characterization of the excited-state potential-energy surface exhibiting two distinct $S_1$ and $S_x$ potential minima separated from the FC region by two most likely orthogonal reaction coordinates, along which the system evolves into two distinct decay channels. No emission associated with a previously identified transient photoproduct state could be observed, indicating the nonemissive nature of this state. In order to illuminate the very fast processes leading to the motion of the excited-state population out of the originally photoexcited FC point and the corresponding reaction coordinates, emission-sensitive experiments with improved (sub 100 fs) time-resolution are necessary. How the complicated dynamics of Pchlide a in solution relates to the initial photochemistry of Pchlide a bound to the enzyme POR is the subject of our future work.

  

## Experimental Section

Pchlide a was isolated from five-day old, dark-grown oat seedlings (*Secale cereale* L. cv Tomba) fed with 15 mM 5-aminolevulinic acid according to a slightly modified literature method.[28] In brief, the tips of the coleoptiles (100 g) were disrupted by homogenization in a Waring blender and the Pchlide a was extracted into an ice-cold 10 mM Tricin buffer (pH 7.5) containing 75% (v/v) acetone (400 mL). After centrifugation, the pigment was extracted into diethyl ether (400 mL). Following the addition of *n*-hexane (400 mL), Pchlide a was extracted with a 4:1 mixture of methanol and 0.01 M ammonia and repeatedly washed with a 1:1 mixture of diethyl ether and *n*-hexane. In a subsequent procedure, Pchlide a was transferred into diethyl ether again by extraction of the methanolic solution with a 1:3 mixture of $H_2O$ and diethyl ether. Finally, the diethyl ether phase was dried with $Na_2SO_4$ and evaporated under a slow stream of nitrogen. After preparation, pure samples of Pchlide a were stored in the dark at 250 K until use. The purity of the isolated Pchlide a was checked by analytical high-performance liquid chromatography (HPLC) using a Hewlett-Agilent 1100 apparatus equipped with a LCQ mass spectrometer (Finnigan). Pchlide a was separated on a reverse-phase C18 column in a 50–100% acetonitrile gradient with the addition of 0.1% trifluoroacetic acid and eluted with a *m/z* peak of 591.7 g mol$^{-1}$. This *m/z* peak corresponds with the molecular mass expected for Pchlide a when it is taken into account that, under the separation conditions, the $Mg^{2+}$ is lost.

For the time-resolved fluorescence measurements, samples of Pchlide a were freshly dissolved in the desired solvent to give an optical density (OD) of 0.1 in a 1 mm optical path length at the excitation wavelength. Pchlide a was excited at 398 nm using the frequency-doubled output of a Ti:Sapphire laser. The oscillator (Spectra Physics) produced 100 fs (FWHM) pulses at a repetition rate of 80 MHz. The fluorescence spectra were recorded using a spectrograph (Chromex 250IS) and a streak camera (Hamamatsu C6860). The fluorescence spectra were recorded up to 2 ns after excitation with 40 ps (FWHM of the experimental response function) time resolution, or up to 100 ps with a time resolution of $\approx$2 ps (FWHM). The spectral windows employed in the measurements presented here were 100 nm wide. A polarizer placed in front of the spectrometer entrance slit was used in combination with a Berek Compensator placed in front of the sample to obtain magic-angle fluorescence kinetics. For the measurements, the sample was placed into a rotating cuvette in order to avoid sample damage. The integrity of the sample was controlled by repeatedly measuring the steady-state absorption spectra. For the measurement of the fluorescence kinetics on the nanosecond timescale, another experimental setup was used. In this case, the sample was excited by the frequency-doubled output of a Ti:Sapphire laser at 435 nm at a repetition rate of 0.8 or 4 MHz. The time- and wavelength-resolved fluorescence signal was collected using a streak camera (Hamamatsu C4334) in combination with an imaging monochromator (Chromex 250IS). The resulting image from the streak camera was collected in photon-counting mode.[29] This setup allows for a time resolution of about 30 and 200 ps at scanning ranges of 1 ns and 20 ns, respectively.

## *Acknowledgements*

*We thank Swati De and Tero Kesti for their assistance. This work was financially supported by the Deutsche Forschungsgemeinschaft, through the grant Sonderforschungsbereich 436 (Metallvermittelte Reaktionen nach dem Vorbild der Natur, TP C1). The work at Lund University was performed with financial support by the Deutscher Akademischer Austausch Dienst. B.D. gratefully acknowledges the financial support by the Studienfonds der Chemischen Industrie.*

**Keywords:** femtochemistry · fluorescence spectroscopy · photochemistry · porphyrins · time-resolved spectroscopy

[1] J. Y. Suzuki, D. W Bolivar, C. E. Bauer, *Annu. Rev. Genet.* **1997**, *31*, 3161.
[2] S. Beale, *Photosynth. Res.* **1999**, *60*, 43–73.
[3] J. E. Cornah, M. J. Terry, A. G. Smith, *Trends Plant Sci.* **2003**, *8*, 224–230.
[4] U. Eckhardt, B. Grimm, S. Hörtensteiner, *Plant Mol. Biol.* **2004**, *56*, 1–14.
[5] M. Moulin, A. G. Smith, *Biochem. Soc. Trans.* **2005**, *33*, 737–742.
[6] N. S. Beer, W. T. Griffiths, *Biochem. J.* **1981**, *195*, 83–92.
[7] J. Y. Suzuki, C. E. Bauer, *Proc. Natl. Acad. Sci. USA* **1995**, 3749–3753.
[8] H. M. Wilks, M. P. Timko, *Proc. Natl. Acad. Sci. USA* **1995**, 724–728.
[9] W. Rüdiger, in *The Porphyrin Handbook* (Eds.: K. M. Kadish, K. M. Smith, R. Guilard), Academic Press, Amsterdam, **2003**, Vol. 13, p. 71.
[10] B. Schoefs, F. Franck, *Photochem. Photobiol.* **2003**, *78*, 543–557.
[11] T. Masuda, K. Takamiya, *Photosynth. Res.* **2004**, *81*, 1–29.
[12] J. Yang, Q. Cheng, *Plant Biol.* **2004**, *6*, 537–544.
[13] D. J. Heyes, C. N. Hunter, I. H. M. van Stokkum, R. van Grondelle, *Nat. Struct. Biol.* **2003**, *10*, 491–492.
[14] B. Dietzek, W. Kiefer, J. Popp, G. Hermann, M. Schmitt, *J. Phys. Chem. B* **2006**, *110*, 4399–4406.
[15] B. Dietzek, R. Maksimenka, T. Siebert, E. Birckner, W. Kiefer, J. Popp, G. Hermann, M. Schmitt, *Chem. Phys. Lett.* **2004**, *397*,110–115.
[16] M. Gouterman, in *The Porphyrins*, Vol. 3 (Ed.: D. Dolphin), Academic Press, New York, **1978**, p. 1.
[17] B. Mysliwa-Kurdziel, J. Kruk, K. Strzalka, *Photochem. Photobiol.* **2004**, *79*, 62–67.
[18] T. Elsaesser, W. Kaiser, *Annu. Rev. Phys. Chem.* **1991**, 42, 83–107.
[19] M. L. Horng, J. A. Gardecki, A. Papazyan, M. Maroncelli, *J. Phys. Chem.* **1995**, *99*, 17311–17337.
[20] H. Z. Yu, J. S. Baskin, A. H. Zewail, *J. Phys. Chem. A* **2002**, *106*, 9845–9854.
[21] J. S. Baskin„ H. Z. Yu, A. H. Zewail, *J. Phys. Chem. A* **2002**, *106*, 9837–9844.
[22] B. Dietzek, R. Maksimenka, W. Kiefer, G. Hermann, J. Popp, M. Schmitt, *Chem. Phys. Lett.* **2005**, *415*, 94–99.
[23] T. Polivka, V. Sundstrom, *Chem. Rev.* **2004**, *104*, 2021–2071.
[24] D. J. Heyes, A. V. Ruban, H. M. Wilks, C. N. Hunter, *Proc. Natl. Acad. Sci. USA* **2002**, *99*, 11145–11150.
[25] D. J. Heyes, C. N. Hunter, *Biochem.* **2004**, *43*, 8265–8271.
[26] V. I. Raskin, A. Schwartz, *Photosynth. Res.* **2002**, 74, 181–186.
[27] D. J. Heyes, C. N. Hunter, *Trends Biochem. Sci.* **2005**, *30*, 642–649.
[28] H. Klement, M. Helfrich, U. Oster, S. Schoch, W. Rüdiger, *Eur. J. Biochem.* **1999**, *265*, 862–874.
[29] The absolute wavelength numbers of the fluorescence given in the paper correspond to the calibration and correction curves as established for the various experimental setups (steady-state fluorescence spectrometer and the two different streak camera setups). These experiments were not cross-calibrated, and calibrations and corrections might have shifted over time. Thus, slight differences in absolute values for the emission maxima as obtained from various experiments might be attributed to these experimental uncertainties.

Received: March 23, 2006
Published online on July 14, 2006

  